Check for updates

Double-ratiometric fluorescence imaging of H_2Se and $O_2^{·-}$ under hypoxia for exploring Na_2SeO_3-induced HepG2 cells' apoptosis†

Xiaonan Gao, [iD] ‡ Wenfei Guo,‡ Lihong Ge, Fanpeng Kong, Kehua Xu* and Bo Tang [iD] *

Sodium selenite (Na_2SeO_3), as an anti-tumor drug for inducing tumor cells' apoptosis, has been widely studied under normoxic conditions and has been shown to exhibit oxidative stress process-induced apoptosis. However, since the real tumor environment is hypoxic, the actual mechanism is still unclear. Hence, considering the main metabolite of Na_2SeO_3 in the metabolic process to be hydrogen selenide (H_2Se) and also that it can be converted to superoxide anion ($O_2^{·-}$) instantaneously in the presence of oxygen, a dual-ratiometric fluorescence imaging system for simultaneous monitoring of the changes of H_2Se and $O_2^{·-}$ induced by Na_2SeO_3-guided tumor cell apoptosis under hypoxic conditions was constructed. Two molecular probes NIR-H_2Se and dihydroethidium were used to detect H_2Se and $O_2^{·-}$, respectively, whereas Rhodamine 110 was used as the reference fluorophore. Notably, H_2Se levels significantly increased under hypoxic conditions, but there was no change in the level of $O_2^{·-}$, which is inconsistent with the results of the previous researches. Therefore, we hypothesize that the mechanism of Na_2SeO_3-induced apoptosis for tumor cells is caused by reductive stress; also, this method can be applied for the future study of other anti-cancer selenium compounds.

Introduction

Selenium,[1,2] as a common protective agent against cancer, can effectively reduce the morbidity and mortality of tumors including lung cancer, colorectal cancer, lymphoma, and prostate cancer.[3–5] The evidence from latent periods, clinical stages and epidemiology supports the chemopreventive role of selenium.[6–8] Therefore, sodium selenite (Na_2SeO_3) has recently become the research hotspot as an anti-cancer medicine due to its high efficiency, low toxicity and cost-effectiveness. However, the precise anti-cancer mechanism of how Na_2SeO_3 can induce tumor cell apoptosis remains poorly understood. To date, research has been done on tumor cell cultures with Na_2SeO_3 under normoxic conditions. It shows that the most generally accepted mechanism for Na_2SeO_3 treatment is by cell apoptosis induced by elevating the reactive oxygen species (ROS) levels and the involvement of oxidative stress.[9–12] Specifically, hydrogen selenide (H_2Se) is the key small molecule metabolite

College of Chemistry, Chemical Engineering and Materials Science, Key Laboratory of Molecular and Nano Probes, Ministry of Education, Collaborative Innovation Center of Functionalized Probes for Chemical Imaging in Universities of Shandong, Shandong Normal University, Jinan 250014, P. R. China. E-mail: Xukehua@sdnu.edu.cn; Tangb@sdnu.edu.cn

of Na_2SeO_3 in vivo, and it reacts with O_2 to produce and accumulate a large amount of ROS (mainly the superoxide anion, $O_2^{·-}$), resulting in tumor cell oxidative stress, which leads to apoptosis.[13–16] Nevertheless, since the tumor microenvironment is hypoxic ($0.7–1.8\%$ O_2)[17] due to the rapid proliferation of cancer cells and imbalance of new blood vessel formation,[18–20] it is still a great challenge to understand the anti-cancer mechanism in hypoxic conditions, which needs to be solved urgently.

To clarify the mechanism, fluorescent probes, which are promising detection tools[21] due to their non-invasiveness, high sensitivity, selectivity, rapid response, and high spatial resolution,[22–28] are the primary option. Unfortunately, these fluorescent probes are limited by environmental conditions, probe distribution, and instrument performance, thereby only showing changes in emission intensities.[29,30] In contrast, ratiometric probes, using the ratio of two different emission wavelengths as the detection signal, provide a built-in correction to the above factors for a more accurate analysis.[31–34]

In this regard, a double-ratiometric method for simultaneous fluorescence imaging analysis to monitor the changes in H_2Se and $O_2^{·-}$ levels in tumor cells was developed. The method studies the apoptosis process induced by pharmacological doses of Na_2SeO_3 in hypoxic conditions. Herein, we chose the fluorescence probe (NIR-H_2Se, $\lambda_{ex}/\lambda_{em} = 688/735$ nm) designed by our group[35] and the commercial fluorescence probe (dihydroethidium, $\lambda_{ex}/\lambda_{em} = 370/420$ nm)[36,37] to monitor the changes in intracellular H_2Se and $O_2^{·-}$ concentrations in both normoxic

conditions and hypoxic conditions, respectively. Meanwhile, Rhodamine 110 ($\lambda_{ex}/\lambda_{em}$ = 496/532 nm) was chosen as a reference fluorophore. This method could potentially avoid the influences of certain external factors on detection accuracy including environmental conditions, light scattering and probe distribution, therefore improving the detection accuracy of the target molecules *in vivo*.[38,39]

Experimental

Materials

All chemicals were analytical-reagent grade and all solvents were purified by a conventional method before use. Rhodamine 110 was purchased from J&K (China). The NIR-H_2Se probe was synthesized in our laboratory following a previous protocol.[35] Dihydroethidium (DHE) and KO_2 were purchased from Aladdin (China). Stock solutions (1 mM) for probes were prepared by dissolving probe in DMSO (Sigma-Aldrich). Sartorius ultrapure water (18.2 MΩ cm) was used throughout the experiments. H_2Se was prepared by reacting Al_2Se_3 with H_2O under an N_2 atmosphere for 30 min at room temperature before use every time.[40,41] $O_2^{\bullet-}$ was generated from KO_2 in DMSO or xanthine oxidase. Na_2SeO_3 was purchased from Sigma-Aldrich. Dulbecco's Modified Eagle Medium (DMEM) was obtained from British Biotechnology (China). HepG2 cells were purchased from the Committee on Type Culture Collection of the Chinese Academy of Sciences.

Instruments

The fluorescence spectra measurements were performed with an FLS-920 Fluorescence Spectrometer (Edinburgh, UK). The fluorescence imaging of cells was recorded on a TCS SP5 confocal laser scanning microscope with an objective lens (×40) (Leica, Germany). The cells were cultured in a 5% CO_2/95% air incubator MCO-15 AC (Sanyo, Japan).

Fluorescence spectra measurements

Ten μM probe NIR-H_2Se was mixed with 5 μM probe DHE, 1 μM Rhodamine 110 and 10 mM PBS (pH = 7.4); then, various amounts of H_2Se (0, 1, 2, 4, 6, 8, 9, 10, 11 μM) were added. The fluorescence intensities were measured at $\lambda_{ex}/\lambda_{em}$ = 496/532 nm and $\lambda_{ex}/\lambda_{em}$ = 688/735 nm. For a parallel study, 5 μM probe DHE was mixed with 10 μM probe NIR-H_2Se, 1 μM Rhodamine 110 and 10 mM PBS (pH = 7.4) and then, various amounts of $O_2^{\bullet-}$ (0, 1, 2, 3, 4, 5, 6, 7, 8 μM) were added for fluorescence measurements at $\lambda_{ex}/\lambda_{em}$ = 496/532 nm and $\lambda_{ex}/\lambda_{em}$ = 488/638 nm.

Cell culture

HepG2 cells in the exponential phase of growth were used for the cell experiments. The concentrations of the counted cells were adapted to 1×10^6 cells per mL for confocal fluorescence imaging with a culture medium. The cells were cultured with DMEM and supplemented with 1% antibiotics (100 U mL^{-1} penicillin and 100 mg mL^{-1} streptomycin) and 10% fetal bovine serum (FBS) at 37 °C under a humidified atmosphere of 5%

CO_2/95% air (20% O_2), 75% CO_2/25% air (5% O_2) and 95% CO_2/5% air (1% O_2) for normoxic and hypoxic conditions in an MCO-15AC incubator, respectively.

Confocal fluorescence imaging

HepG2 cells were prepared in glass-bottom culture dishes and cultured for 24 h. One group of cells without treatment of Na_2SeO_3 served as the control group and the other groups were treated with various amounts of Na_2SeO_3 (2, 5, 10 μM) for 12 h under either normoxic or hypoxic conditions. All groups were further incubated in an FBS-free culture medium mixed with 10 μM probe NIR-H_2Se, 5 μM probe DHE and 1 μM Rhodamine 110 at 37 °C for 15 min and then washed with PBS (pH = 7.4, 10 mM) three times. Afterwards, the cells were imaged immediately using a confocal microscope with an objective lens (×40) and examined by CLSM with different laser transmitters. The emitted light intensities were collected with an META detector from 490 to 550 nm, 590 to 670 nm and 690 to 760 nm.

Results and discussion

Spectroscopic properties of NIR-H_2Se with H_2Se, DHE with $O_2^{\bullet-}$ and Rhodamine 110

The excitation and emission spectra of NIR-H_2Se with H_2Se, DHE with $O_2^{\bullet-}$ and Rhodamine 110 were recorded (Fig. S1†). Interestingly, the emission spectra of the reaction products of NIR-H_2Se with H_2Se, DHE plus $O_2^{\bullet-}$, and Rhodamine 110 are located at 735, 638 and 532 nm, respectively. Therefore, the emission spectra of Rhodamine 110 and the two reaction products exhibit a fairly ideal separation effect with approximately 100 nm between each peak, making their simultaneous detection possible (Fig. 1).

Ratiometric detection

The fluorescence responses of DHE to H_2Se and NIR-H_2Se to $O_2^{\bullet-}$ were tested by using the mixture of NIR-H_2Se, DHE and Rhodamine 110 to simultaneously monitor the levels of H_2Se and $O_2^{\bullet-}$. As shown in Fig. 2a, $O_2^{\bullet-}$ (5 μM) yielded a strong fluorescence signal with DHE (5 μM), but high concentrations
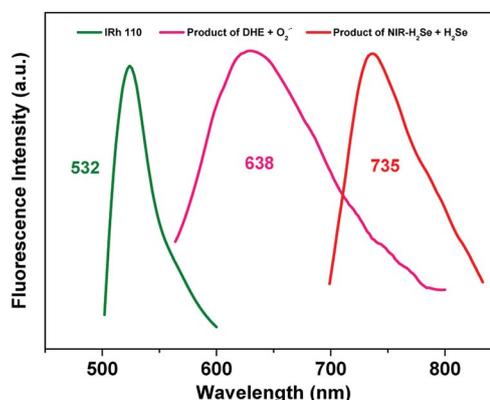
Fig. 1 Fluorescence emission spectra of (red) NIR-H_2Se with H_2Se, (pink) DHE with $O_2^{\bullet-}$ and (green) Rhodamine 110.
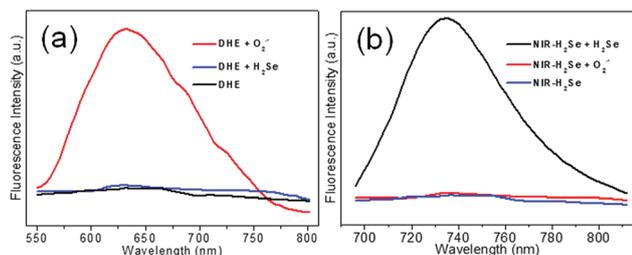
Fig. 2 Interference measurement of (a) DHE to H$_2$Se and (b) NIR-H$_2$Se to O$_2^{\cdot-}$. All of the spectra were acquired at room temperature in 10 mM PBS (pH = 7.4) with (a) $\lambda_{ex}/\lambda_{em}$ = 488/638 nm or (b) $\lambda_{ex}/\lambda_{em}$ = 688/735 nm.

of H$_2$Se (15 μM) did not exhibit a fluorescence response. Similarly, the fluorescence response of NIR-H$_2$Se (10 μM) to O$_2^{\cdot-}$ (10 μM) was negligible, but a strong fluorescence signal was obtained with 10 μM H$_2$Se (Fig. 2b). Then, the optical properties of the probe mixtures with Rhodamine 110 were recorded with various concentrations of H$_2$Se in simulated physiological conditions (10 mM PBS, pH = 7.4). The fluorescence intensities increased with increasing concentrations of H$_2$Se at 735 nm (Fig. 3a) but hardly fluctuated at 532 nm (Fig. 3b, black curve, right Y scale). Interestingly, there is a good linear correlation between the fluorescence intensity ratio F_{735}/F_{532} and H$_2$Se concentrations from 0 to 11.0 μM (Fig. 3b, red curve, left Y scale). The equation of linear regression is F_{735}/F_{532} = 0.23 + 0.17 [H$_2$Se] μM with the R value of 0.9937, indicating that the fluorescence intensity ratio F_{735}/F_{532} increased with increasing concentrations of H$_2$Se linearly. Simultaneously, similar
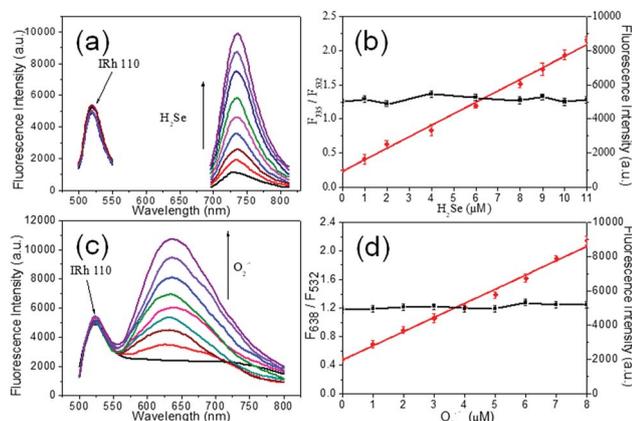
fluorescence responses of the mixture towards O$_2^{\cdot-}$ under various concentrations of O$_2^{\cdot-}$ in simulated physiological conditions (10 mM PBS, pH = 7.4) were also obtained (Fig. 3c); the fluorescence intensity was significantly enhanced *via* increasing O$_2^{\cdot-}$ concentrations at 638 nm but was maintained at 532 nm (Fig. 3d, black curve, right Y scale). Also, a linear correlation between the fluorescence intensity ratio F_{638}/F_{532} and O$_2^{\cdot-}$ concentrations from 0 to 8.0 μM (Fig. 3d, red circles, left Y scale) was observed. The equation of linear regression is F_{638}/F_{532} = 0.47 + 0.20 [O$_2^{\cdot-}$] μM with the R value of 0.9923, indicating that the fluorescence intensity ratio of F_{638}/F_{532} increased linearly with increasing concentrations of O$_2^{\cdot-}$. Overall, the results demonstrated that it is entirely feasible to use NIR-H$_2$Se and DHE for simultaneously monitoring the changes in H$_2$Se and O$_2^{\cdot-}$ in a complex system.

Co-staining imaging in living cells

To further test the simultaneous imaging of H$_2$Se and O$_2^{\cdot-}$ *in vitro*, co-staining experiments were carried out. Since Na$_2$SeO$_3$ metabolite H$_2$Se is mainly accumulated in the liver, the cell model HepG2 was selected for the following study. HepG2 cells were first incubated in FBS-free culture medium mixed with 10 μM NIR-H$_2$Se, 5 μM DHE and 1 μM Rhodamine 110 at 37 °C for 15 min and then, confocal fluorescence images were obtained. Fig. 4 displays the distribution of Rhodamine 110 (green), the product of DHE with native O$_2^{\cdot-}$ of HepG2 cells (yellow), the product of NIR-H$_2$Se with H$_2$Se (red), and the merged image. The two probes and the reference achieved excellent spectral separation in the cell as well as great biocompatibility. The two probes' reaction products and the reference molecular structure all contain two amino groups, making the degree of impact by the intracellular complex environment almost the same, which further improved the sensitivity of the detection. Hence, the mixture of NIR-H$_2$Se, DHE and Rhodamine 110 can be used to simultaneously recognize H$_2$Se and O$_2^{\cdot-}$ in living cells.

Double-ratiometric simultaneous detection under normoxia and hypoxia

For the next step, the probe mixture was applied to explore its application for double-ratiometric, simultaneous imaging of endogenous H$_2$Se and O$_2^{\cdot-}$ in HepG2 cells pre-treated with Na$_2$SeO$_3$ under normoxic (20% O$_2$) and hypoxic (5% O$_2$, 1% O$_2$)

Fig. 3 Ratiometric detection with the mixture of 10 μM NIR-H$_2$Se, 5 μM DHE and 1 μM Rhodamine 110 toward H$_2$Se and O$_2^{\cdot-}$. (a) Fluorescence response of the mixture to various concentrations (0 to 11.0 μM) of H$_2$Se. (b) The linear correlation between the fluorescence intensity ratio F_{735}/F_{532} and H$_2$Se concentrations (red) and fluorescence intensities changes of Rhodamine 110 to H$_2$Se concentrations (black). (c) Fluorescence response of the mixture to various concentrations (0 to 8.0 μM) of O$_2^{\cdot-}$. (d) The linear correlation between the fluorescence intensity ratio F_{638}/F_{532} and O$_2^{\cdot-}$ concentrations (red) and changes in the fluorescence intensity of Rhodamine 110 to O$_2^{\cdot-}$ concentrations (black). The data shown are representative of repeating experiments (n = 3).

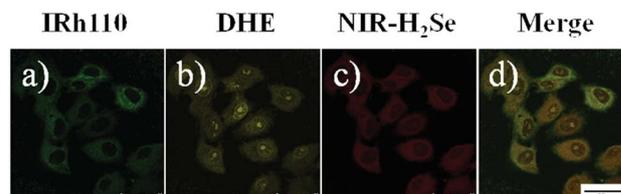**Fig. 4** Co-staining images of HepG2 cells incubated with FBS-free culture medium mixed with 1 μM Rhodamine 110, 5 μM DHE and 10 μM NIR-H$_2$Se at 37 °C for 15 min. The emitted light was collected with an META detector from 490 to 550 nm, 590 to 670 nm and 690 to 760 nm. (a) Green channel. (b) Yellow channel. (c) Red channel. (d) Merge of (a), (b) and (c). Scale bar = 50 μm.

conditions. One group of HepG2 cells without treatment of Na_2SeO_3 served as the control group, and the other groups were treated with Na_2SeO_3 (2, 5, 10 μM) for 12 h under either normoxia (20% O_2) or hypoxia (5% O_2, 1% O_2). Afterwards, the cells were incubated in an FBS-free culture medium mixed with 10 μM NIR-H_2Se, 5 μM probe DHE and 1 μM Rhodamine 110 at 37 °C for 15 min. The ratiometric images of H_2Se were achieved by combining the images obtained in the band path of 490–550 nm with the corresponding images in the band path of 690–760 nm. Meanwhile, the concentration of $O_2^{\cdot-}$ was also obtained by combining the images obtained in the band path of 490–550 nm with the corresponding images in the band path of 590–670 nm (Fig. 5 and S2–S4†). Fig. 5a shows that under different oxygen concentrations, the concentration of H_2Se in HepG2 cells increased by the Na_2SeO_3 concentration. From the quantitative map, it can be seen that with the decrease in oxygen concentration and increase in Na_2SeO_3 concentration, the H_2Se content gradually increased. At 1% O_2, the concentration of H_2Se in the HepG2 cells was relatively high with 10 μM Na_2SeO_3 (Fig. 5b). Consequently, under different oxygen concentrations, the content of $O_2^{\cdot-}$ in the HepG2 cells increased while increasing Na_2SeO_3 since the increase of oxygen and Na_2SeO_3 led to gradually rising $O_2^{\cdot-}$ levels (Fig. 5c). At 20% O_2, the concentration of $O_2^{\cdot-}$ in the HepG2 cells was relatively high with 10 μM Na_2SeO_3 incubation, but the content of $O_2^{\cdot-}$ in the HepG2 cells remained unchanged under the condition of 1% O_2 (Fig. 5d).

In this regard, higher H_2Se contents were observed in hypoxic environments rather than in normoxic conditions in parallel experiments. Correspondingly, lower $O_2^{\cdot-}$ contents were maintained and they hardly changed under hypoxic environments, whereas $O_2^{\cdot-}$ contents gradually increased in the HepG2 cells with Na_2SeO_3 in a time- and dose-dependent manner under normoxic conditions. These results indicate that the Na_2SeO_3 anticancer mechanism is not an ROS-induced apoptosis process under hypoxic conditions. Thus, the anticancer effect of Na_2SeO_3 in solid tumors should be reductive stress to trigger cell death of cancer cells.

Conclusions

In summary, we developed a novel double-ratiometric fluorescence probe system for simultaneous fluorescence imaging analysis of the changes in H_2Se and $O_2^{\cdot-}$ levels in the tumor cell HepG2's apoptosis process induced by pharmacological doses of Na_2SeO_3. The system verifies that the content of $O_2^{\cdot-}$ is clearly higher in the tumor cell apoptosis process induced by Na_2SeO_3 in normoxic conditions, and H_2Se is almost completely oxidized by O_2 to produce $O_2^{\cdot-}$. In contrast, under hypoxic conditions, the $O_2^{\cdot-}$ content is extremely low, but the H_2Se content increases dramatically. Therefore, in solid tumors, the anti-cancer mechanism of Na_2SeO_3 can be ascribed to reductive stress induced by H_2Se but not oxidative stress. This finding will significantly improve the investigation of the anti-cancer mechanism of Na_2SeO_3, and the double-ratiometric fluorescence method can be used as a suitable tool for the study of other selenium compounds in the future.

Conflicts of interest

There are no conflicts to declare.

Acknowledgements

References

1 J. Chen, Y. Zhu and Y. Zhang, *RSC Adv.*, 2016, **6**, 62193–62199.

2 Y. Nan, W. Zhao, X. Xu, C.-T. Au and R. Qiu, *RSC Adv.*, 2015, **5**, 69299–69306.

3 Y. Cui, S. Vogt, N. Olson, A. G. Glass and T. E. Rohan, *Cancer Epidemiol., Biomarkers Prev.*, 2007, **16**, 1682–1685.

4 T. Chen and Y.-S. Wong, *Int. J. Biochem. Cell Biol.*, 2009, **41**, 666–676.

5 I. A. Asfour, M. M. El-Tehewi, M. H. Ahmed, M. A. Abdel-Sattar, N. N. Moustafa, H. M. Hegab and O. M. Fathey, *Biol. Trace Elem. Res.*, 2009, **127**, 200–210.

6 R. Sinha and k. El-Bayoumy, *Curr. Cancer Drug Targets*, 2004, **4**, 13–28.

7 L. C. Clark, B. Dalkin, A. Krongrad, G. F. Combs Jr, B. W. Turnbull, E. H. Slate, R. Witherington, J. H. Herlong, E. Janosko, D. Carpenter, C. Borosso, S. Falk and J. Rounder, *Br. J. Urol.*, 1998, **81**, 730–734.
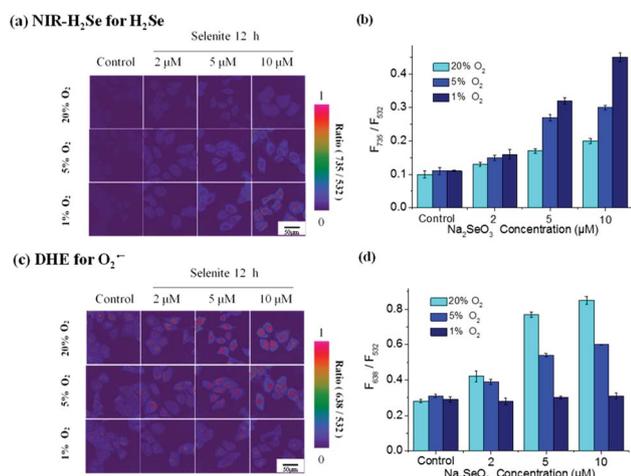
Fig. 5 Confocal fluorescence double-ratiometric images of endogenous H_2Se and $O_2^{\cdot-}$ in living HepG2 cells treated with various concentrations of Na_2SeO_3 under normoxic and hypoxic conditions. (a) The fluorescence ratio image (F_{735}/F_{532}). (b) The corresponding statistic fluorescence ratio (F_{735}/F_{532}) for (a). (c) The fluorescence ratio image (F_{638}/F_{532}). (d) The corresponding statistic fluorescence ratio (F_{638}/F_{532}) for (c). The images shown are representative of repeated experiments ($n = 3$). Scale bar = 50 μm.

8 Y. Xia, C. Wang, T. Xu, Y. Li, M. Guo, Z. Lin, M. Zhao and B. Zhu, *RSC Adv.*, 2018, **8**, 1917–1926.

9 H.-M. Shen, C.-F. Yang and C.-N. Ong, *Int. J. Cancer*, 1999, **81**, 820–828.

10 G. Nilsonne, X. Sun, C. Nyström, A.-K. Rundlöf, A. P. Fernandes, M. Björnstedt and K. Dobra, *Free Radical Biol. Med.*, 2006, **41**, 874–885.

11 L. Guan, B. Han, Z. Li, F. Hua, F. Huang, W. Wei, Y. Yang and C. Xu, *Apoptosis*, 2009, **14**, 218–225.

12 J. J. An, K. J. Shi, W. Wei, F. Y. Hua, Y. L. Ci, Q. Jiang, F. Li, P. Wu, K. Y. Hui, Y. Yang and C. M. Xu, *Cell Death Dis.*, 2013, **4**, 973–982.

13 H. Luo, Y. Yang, F. Huang, F. Li, Q. Jiang, K. Shi and C. Xu, *Cancer Lett.*, 2012, **315**, 78–85.

14 S.-H. Park, J.-H. Kim, G. Y. Chi, G.-Y. Kim, Y.-C. Chang, S.-K. Moon, S.-W. Nam, W.-J. Kim, Y. H. Yoo and Y. H. Choi, *Toxicol. Lett.*, 2012, **212**, 252–261.

15 X. Liu, B. Hu, R. Cheng, F. Kong, X. Pan, K. Xu and B. Tang, *Chem. Commun.*, 2016, **52**, 6693–6696.

16 B. Hu, R. Cheng, X. Liu, X. Pan, F. Kong, W. Gao, K. Xu and B. Tang, *Biomaterials*, 2016, **92**, 81–89.

17 S. Rey, L. Schito, M. Koritzinsky and B. G. Wouters, *Adv. Drug Delivery Rev.*, 2017, **109**, 45–62.

18 P. Vaupel, F. Kallinowski and P. Okunieff, *Cancer Res.*, 1989, **49**, 6449–6465.

19 D. Hanahan and R. A. Weinberg, *Cell*, 2000, **100**, 57–70.

20 M. C. Hung, G. B. Mills and D. Yu, *Nat. Med.*, 2009, **15**, 246–247.

21 E. Zhang, P. Ju, P. Guo, X. Hou, X. Hou, H. Lv, J.-j. Wang and Y. Zhang, *RSC Adv.*, 2018, **8**, 31658–31665.

22 T. Ueno and T. Nagano, *Nat. Methods*, 2011, **8**, 642–645.

23 L. L. Zhang, H. K. Zhu, C. C. Zhao and X. F. Gu, *Chin. Chem. Lett.*, 2017, **28**, 218–221.

24 F. Wang, Y. Zhu, L. Zhou, L. Pan, Z. Cui, Q. Fei, S. Luo, D. Pan, Q. Huang, R. Wang, C. Zhao, H. Tian and C. Fan, *Angew. Chem., Int. Ed.*, 2015, **54**, 7349–7353.

25 C. Zhao, X. Zhang, K. Li, S. Zhu, Z. Guo, L. Zhang, F. Wang, Q. Fei, S. Luo, P. Shi, H. Tian and W. H. Zhu, *J. Am. Chem. Soc.*, 2015, **137**, 8490–8498.

26 J. Xu, J. Pan, X. Jiang, C. Qin, L. Zeng, H. Zhang and J. F. Zhang, *Biosens. Bioelectron.*, 2016, **77**, 725–732.

27 X. Cheng, H. Jia, J. Feng, J. Qin and Z. Li, *Sens. Actuators, B*, 2013, **184**, 274–280.

28 X. Gu, C. Liu, Y. C. Zhu and Y. Z. Zhu, *J. Agric. Food Chem.*, 2011, **59**, 11935–11939.

29 X. Liu, Q. Yang, W. Chen, L. Mo, S. Chen, J. Kang and X. Song, *Org. Biomol. Chem.*, 2015, **13**, 8663–8668.

30 L. Yuan, W. Lin, Y. Xie, B. Chen and J. Song, *Chem.–Eur. J.*, 2012, **18**, 2700–2706.

31 L. Yuan, W. Lin, J. Song and Y. Yang, *Chem. Commun.*, 2011, **47**, 12691–12693.

32 X. Jiang, J. Xu, Y. Zhang, H. Wang, L. Zeng and Y. Zhang, *Anal. Methods*, 2016, **8**, 1572–1576.

33 L. Zhu, J. Xu, Z. Sun, B. Fu, C. Qin, L. Zeng and X. Hu, *Chem. Commun.*, 2015, **51**, 1154–1156.

34 Z. Ye, C. Duan, R. Sheng, J. Xu, H. Wang and L. Zeng, *Talanta*, 2018, **176**, 389–396.

35 F. Kong, L. Ge, X. Pan, K. Xu, X. Liu and B. Tang, *Chem. Sci.*, 2016, **7**, 1051–1056.

36 Z. Yu, Q. Sun, W. Pan, N. Li and B. Tang, *ACS Nano*, 2015, **9**, 11064–11074.

37 R. M. Monaghan, R. G. Barnes, K. Fisher, T. Andreou, N. Rooney, G. B. Poulin and A. J. Whitmarsh, *Nat. Cell Biol.*, 2015, **17**, 782–792.

38 K. Komatsu, Y. Urano, H. Kojima and T. Nagano, *J. Am. Chem. Soc.*, 2007, **129**, 13447–13454.

39 D. Srikun, E. W. Miller, D. W. Domaille and C. J. Chang, *J. Am. Chem. Soc.*, 2008, **130**, 4596–4597.

40 C. Mealli, S. Midollini and L. Sacconi, *Inorg. Chem.*, 1978, **17**, 632–637.

41 V. V. Matylitsky, A. Shavel, N. Gaponik, A. Eychmüller and J. Wachtveitl, *J. Phys. Chem. C*, 2008, **112**, 2703–2710.